ISSN 1846-6168 (Print), ISSN 1848-5588 (Online)
https://doi.org/10.31803/tg-20191031094436

Original scientific paper

Energy Loss Analysis at the Gland Seals of a Marine Turbo-Generator Steam Turbine

Lino Kocijel, Igor Poljak, Vedran Mrzljak, Zlatan Car

Abstract: The paper presents an analysis of marine Turbo-Generator Steam Turbine (TGST) energy losses at turbine gland seals. The analyzed TGST is one of two identical Turbo-Generator Steam Turbines mounted in the steam propulsion plant of a commercial LNG carrier. Research is based on the TGST measurement data obtained during exploitation at three different loads. The turbine front gland seal is the most important element which defines TGST operating parameters, energy losses and energy efficiencies. The front gland seal should have as many chambers as possible in order to minimize the leaked steam mass flow rate, which will result in a turbine energy losses' decrease and in an increase in energy efficiency. The steam mass flow rate leakage through the TGST rear gland seal has a low or negligible influence on turbine operating parameters, energy losses and energy efficiencies. The highest turbine energy efficiencies are noted at a high load – on which TGST operation is preferable.

Keywords: energy loss; gland seal; marine steam turbine; turbine efficiency

1 INTRODUCTION

Today, by taking into account the entire world fleet, the dominant power producers for ship propulsion are marine slow speed two-stroke diesel engines [1]. Several authors have proposed improvement of such engines by using various additives in heavy fuel oil [2], by using alternative fuel mixtures with heavy fuel oil [3, 4] or by using several water injection techniques [5]. Middle speed and fast speed four-stroke diesel engines are also used in marine propulsion plants, usually for the electricity generator drive or for other plant needs [6].

In general usage, marine steam propulsion can rarely be found, but due to the specificity of its operation, steam plants are still dominant in the propulsion of LNG (Liquefied Natural Gas) carriers [7, 8]. Power plants which are nowadays used for LNG carrier propulsion (steam and other plants) are complex systems [9] which usually require power management and a maintenance software [10], as well as multi-objective decision support systems [11].

This paper presents an analysis of marine Turbo-Generator Steam Turbine (TGST) energy losses at gland seals. The analyzed TGST is mounted in the steam propulsion plant of a commercial LNG carrier. Based on measurement results at three TGST loads, various distributions of cumulative steam mass flow rate lost through both gland seals were performed. The influences of an increase in the steam mass flow rate which leaked through front gland seal on TGST developed power, energy power losses and energy efficiencies were investigated. The mechanical efficiency of the investigated steam turbine at all observed loads is also taken into account. Based on the obtained results are presented recommendations for TGST operation.

2 DESCRIPTION OF THE ANALYZED MARINE TGST AND THE STEAM POWER PLANT IN WHICH IT OPERATES

In this paper, a marine TGST which operates in a steam propulsion system of a commercial LNG carrier (main specifications of an LNG carrier are presented in Tab. 1) is analyzed. The marine TGST is a low-power steam turbine which drives an electricity generator. In an LNG carrier steam propulsion plant, two identical Turbo-Generator Steam Turbines are mounted, and they always operate parallelly because electricity supply should always be secured. TGST is a condensing type, low-power steam turbine which consists of nine Rateau stages [12].

Table 1 Main specifications of an LNG carrier

Gross tonnage	100 450 tons
Deadweight	84 812 tons
Length	288 m
Breadth	44 m
Main propulsion steam turbine	Mitsubishi MS40-2
Steam generators	2 × Mitsubishi MB-4E-KS
TGST	2 × Shinko RGA 92-2

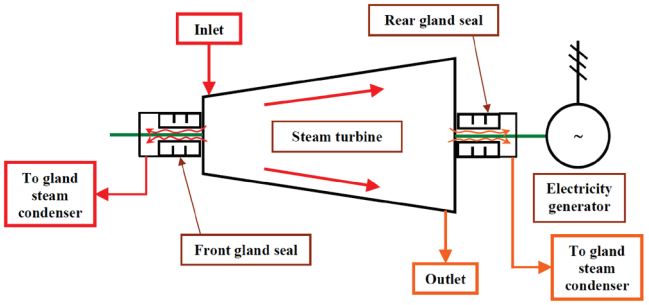

Figure 1 Turbo-Generator Steam Turbine (TGST) scheme with marked steam flow streams

The TGST scheme is presented in Fig. 1. Superheated steam from marine steam generators is delivered directly to all turbines in the marine steam power plant, as well as to both Turbo-Generator Steam Turbines [13] (TGST Inlet, Fig. 1). One small part of the superheated steam delivered to TGST is lost through the front gland seal, while the majority of the delivered steam expanded through nine TGST stages. At the end of steam expansion, one small part of the expanded steam is lost through the rear gland seal, while the rest of the expanded steam exits from TGST to the main marine steam condenser (TGST Outlet, Fig. 1) [14]. Steam gland seals operate in such a manner that they reduce steam

pressure, while steam specific enthalpy (energy content) remains almost constant through the seal [15, 16]. The steam mass flow rate lost through both the front and rear gland seals is led to the gland steam condenser. The mechanical energy produced in TGST stages is delivered to an electricity generator.

A simplified scheme of the entire marine steam propulsion plant from the commercial LNG carrier is presented in Fig. 2 [17]. The majority of marine steam power plant components are the same as in land-based steam power plants [18, 19], but the operation of a marine steam plant must be much more dynamic. Along with the already mentioned two identical Turbo-Generator Steam Turbines, the marine steam system also consists of two identical steam generators [20] in front of which forced draft fans [21] and air heaters (air is heated with steam) [22] are mounted. The main propulsion turbine is composed of two cylinders (high pressure and low pressure) [23], which drive the main propulsion propeller through a marine gearbox. After expansion in all marine turbines, steam condenses in the main condenser and the obtained condensate is delivered to steam generators through a condensate/feed water heating system [24, 25] by using pumps [26].

Components in marine steam power plant, which are not required in land-based steam power plants, are the evaporator (fresh water generator) and desuperheater (which prepare steam extracted from the main turbine for additional heating purposes) [27].

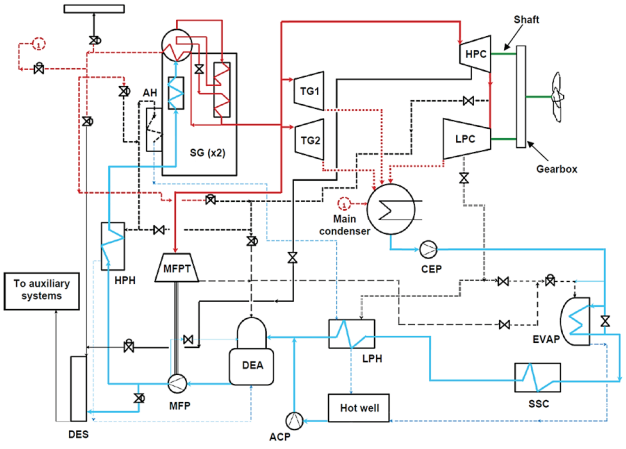

Figure 2 General scheme of a marine steam propulsion plant from the commercial LNG carrier (SG - Steam Generator; AH - Air Heater; TG - Turbo-Generator; HPC - High Pressure Cylinder (main turbine); LPC - Low Pressure Cylinder (main turbine); CEP - Condensate Extraction Pump; EVAP - Evaporator; SSC - Sealing Steam Condenser (Gland steam condenser); LPH - Low Pressure Heater; ACP - Auxiliary Condensate Pump; DEA - Deaerator; MFP - Main Feed-water Pump; MFPT - Main Feed-water Pump Turbine; DES - Desuperheater; HPH - High Pressure Heater)

3 EQUATIONS FOR THE CALCULATION OF ENERGY LOSS THROUGH GLAND SEALS

3.1 General Energy Analysis Equations

The first law of thermodynamics defines the energy analysis of any control volume or system [28, 29]. In a steady state, while disregarding potential and kinetic energy, for a standard control volume can be defined mass and energy balance equations, according to [30, 31]:

$$\sum \dot{m}_{\mathrm{IN}} = \sum \dot{m}_{\mathrm{OUT}} , \tag{1}$$

$$\sum \dot{m}_{\mathrm{IN}} \cdot h_{\mathrm{IN}} - \sum \dot{m}_{\mathrm{OUT}} \cdot h_{\mathrm{OUT}} = P - \dot{Q} . \tag{2}$$

The energy power of a fluid stream flow, according to [32], can be calculated as:

$$\dot{E}_{\mathrm{en}} = \dot{m} \cdot h . \tag{3}$$

The type and operation characteristics of a control volume or system define its energy efficiency. Therefore, each control volume or system can have its form of energy efficiency defined. In general, energy efficiency can be defined with the following equation [33, 34]:

$$\eta_{\mathrm{en}} = \frac{\text{Energy output}}{\text{Energy input}} . \tag{4}$$

3.2 Analyzed TGST Energy Losses through Gland Seals

The mathematical description of energy losses through the TGST front and rear gland seals is based on the conservation of energy. Symbols and markings used in the equations from this section are related to Fig. 1. The energy power input into the analyzed TGST is:

$$\dot{E}_{\mathrm{en,IN,TGST}} = \dot{m}_{\mathrm{inlet}} \cdot h_{\mathrm{inlet}} . \tag{5}$$

The cumulative energy power output from TGST is:

$$\dot{E}_{\mathrm{en,OUT,TGST}} = \dot{m}_{\mathrm{outlet}} \cdot h_{\mathrm{outlet}} + P , \tag{6}$$

with a note that the first part of the Eq. (6) represents the energy power output of steam only.

The energy power loss through the TGST front gland seal is:

$$\dot{E}_{\mathrm{en,PL,FGS}} = \dot{m}_{\mathrm{FGS}} \cdot h_{\mathrm{inlet}} , \tag{7}$$

and the energy power loss through the TGST rear gland seal is:

$$\dot{E}_{\mathrm{en,PL,RGS}} = \dot{m}_{\mathrm{RGS}} \cdot h_{\mathrm{outlet}} . \tag{8}$$

From Eq. (7) and Eq. (8), it should be highlighted that the specific enthalpy of steam which passes through the front gland seal is the same as the steam specific enthalpy at the TGST inlet, while the specific enthalpy of steam which passes through the rear gland seal is the same as the steam specific enthalpy at the TGST outlet.

TGST developed power (which is transferred to the electricity generator) is:

$$P = \left(\dot{m}_{\text{inlet}} - \dot{m}_{\text{FGS}}\right) \cdot \left(h_{\text{inlet}} - h_{\text{outlet}}\right), \tag{9}$$

with a note that Eq. (9) does not take into account the mechanical losses in the power transmission from TGST stages to an electricity generator. If mechanical losses are taken into account, then the Eq. (9) should be multiplied with mechanical efficiency at each observed turbine load. Eq. (9) also defines that the developed TGST power is strongly dependable on the steam mass flow rate lost through the front gland seal, while the steam mass flow rate lost through the rear gland seal do not have any influence on the turbine developed power.

The cumulative steam mass flow rate lost through both TGST gland seals (front and rear) is:

$$\dot{m}_{\text{lost,cumulative}} = \dot{m}_{\text{inlet}} - \dot{m}_{\text{outlet}} = \dot{m}_{\text{FGS}} + \dot{m}_{\text{RGS}}. \tag{10}$$

Without detail measurements of steam mass flow rates lost through the front and rear gland seals, the cumulative steam mass flow rate lost through both gland seals can be distributed in a various ratios between the front and rear gland seal. This fact is used in the performed analysis – various ratios of cumulative steam mass flow rate lost through both gland seals and its distribution to front and rear gland seal are investigated.

The steam mass flow rate lost through the front gland seal (as a share of the cumulative lost steam mass flow rate) is calculated by using the following equation:

$$\dot{m}_{\text{FGS}} = \dot{m}_{\text{lost,cumulative}} \cdot z_{\text{front}}(\%), \tag{11}$$

while the steam mass flow rate lost through the rear gland seal (as a share of the cumulative lost steam mass flow rate) is calculated as:

$$\dot{m}_{\text{RGS}} = \dot{m}_{\text{lost,cumulative}} \cdot z_{\text{rear}}(\%). \tag{12}$$

$z_{\text{front}}(\%)$ in Eq. (11) represents a percentage of the cumulative lost steam mass flow rate through the front gland seal, while $z_{\text{rear}}(\%)$ in Eq. (12) represents a percentage of the cumulative lost steam mass flow rate through the rear gland seal. Energy power loss through both TGST gland seals (energy power loss of the entire TGST) is:

$$\begin{aligned} \dot{E}_{\text{en,PL,TGST}} &= \dot{E}_{\text{en,IN,TGST}} - \dot{E}_{\text{en,OUT,TGST}} = \\ &= \dot{m}_{\text{inlet}} \cdot h_{\text{inlet}} - \dot{m}_{\text{outlet}} \cdot h_{\text{outlet}} - P = . \\ &= \dot{m}_{\text{FGS}} \cdot h_{\text{inlet}} + \dot{m}_{\text{RGS}} \cdot h_{\text{outlet}} \end{aligned} \tag{13}$$

The energy efficiency of the analyzed TGST is:

$$\begin{aligned} \eta_{\text{en,TGST}} &= \frac{P \cdot \eta_{\text{mechanical}}}{\dot{E}_{\text{en,IN,TGST}} - \dot{E}_{\text{en,OUT,TGST}} + P} = \\ &= \frac{P \cdot \eta_{\text{mechanical}}}{\dot{m}_{\text{inlet}} \cdot h_{\text{inlet}} - \dot{m}_{\text{outlet}} \cdot h_{\text{outlet}}} \end{aligned}. \tag{14}$$

The mechanical efficiency of the analyzed TGST in Eq. (14) is assumed as 96 % at high turbine load, 95 % at middle and 94 % at low turbine load (as can be expected for a low-power marine steam turbine [35, 36]).

4 MEASURED AND CALCULATED STEAM OPERATING PARAMETERS AT THE TGST INLET AND OUTLET

The measured steam operating parameters at the TGST inlet are steam temperature, pressure and mass flow rate, while at the TGST outlet, the measured operating parameters are steam temperature and pressure, Tab. 2.

Table 2 Measured and calculated steam operating parameters at the TGST inlet and outlet

Load	Steam at the TGST inlet			
	Temperature (°C)	Pressure (MPa)	Mass flow rate (kg/h)	Steam specific enthalpy (kJ/kg)
High Load	451.5	5.99	5966	3306.7
Middle Load	504.5	6.03	4116	3433.5
Low Load	502.5	6.07	3775	3428.3
Load	Steam at the TGST outlet			
	Temperature (°C)	Pressure (MPa)	Mass flow rate (kg/h)	Steam specific enthalpy (kJ/kg)
High Load	36.83	0.006224	5906.34	2467.3
Middle Load	95.46	0.004224	4074.84	2679.6
Low Load	105.57	0.003974	3737.25	2698.8

Cumulative steam mass flow rate lost through both gland seals (kg/h)		
High Load	Middle Load	Low Load
59.66	41.16	37.75

When the steam mass flow rate lost through turbine gland seals was not taken into consideration, the steam mass flow rate at the turbine inlet is the same as the steam mass flow rate at the turbine outlet. If the steam mass flow rate losses through the turbine gland seals are taken into account, during usual turbine operation, it amounts to about 1 % of the cumulative steam mass flow rate which enters into the turbine (the steam mass flow rate lost through both the front and rear gland seals), regardless of the current turbine load [37]. In the presented analysis, the measurement of steam mass flow rates through the TGST front and rear gland seals or at the TGST outlet were not possible due to the potential problems that the installation of the new measuring equipment could cause. Therefore, it is assumed, as in [37], that the cumulative steam mass flow rate lost through the TGST front and rear gland seals are equal to 1 % of the cumulative steam mass flow rate which enters into the TGST. As a result, the steam mass flow rate at the TGST outlet is calculated as the steam mass flow rate at the TGST inlet

reduced by the cumulative steam mass flow rate lost through both gland seals, Tab. 2.

Steam specific enthalpies at the TGST inlet and outlet, necessary for the energy analysis, are calculated from the known pressures and temperatures at the turbine inlet and outlet by using the NIST-REFPROP 9.0 software [38].

For obtaining measuring results, the measuring equipment already mounted in the LNG carrier steam propulsion plant is used. The measuring equipment at the TGST inlet and outlet is calibrated and used for the control and regulation of TGST during the LNG carrier operation. The list of used measuring devices is presented in Tab. 3, while detailed specifications of each device can be found on the producers' websites.

Table 3 The measuring devices used at the TGST inlet and outlet

Measured operating parameter	Position	Measuring device
Steam temperature	TGST inlet	Greisinger GTF 601-Pt100 - Immersion probe [39]
Steam pressure	TGST inlet	Yamatake JTG980A - Pressure Transmitter [40]
Steam mass flow rate	TGST inlet	Yamatake JTD960A - Differential Pressure Transmitter [41]
Steam temperature	TGST outlet	Greisinger GTF 401-Pt100 - Immersion probe [39]
Steam pressure	TGST outlet	Yamatake JTD910A - Differential Pressure Transmitter [41]

5 THE RESULTS OF ENERGY LOSS ANALYSIS THROUGH TGST GLAND SEALS WITH DISCUSSION

According to the presented equations and steam operating parameters at the TGST inlet and outlet, an analysis of energy losses through the TGST gland seals is performed. Due to the lack of measurement data, several distributions of the cumulative steam mass flow rate lost through both gland seals are observed, as presented in Tab. 4. All presented distributions are observed at each TGST load.

According to the Eq. (9), the TGST developed power is highly influenced by two steam mass flow rates – the first one is the steam mass flow rate at the TGST inlet and the second one is the steam mass flow rate lost through the front gland seal. Tab. 4 presents the increase in the steam mass flow rate lost on the TGST front gland seal which resulted with a decrease in turbine developed power due to the decrease in the steam mass flow rate which expands through the turbine.

From Tab. 4, two conclusions can be derived. The first one is that the TGST front gland seal should be designed with as many chambers as possible within the seal in order to reduce the leaked steam mass flow rate [42, 43]. The second conclusion is that the increase in the steam mass flow rate which leaked through the front gland seal resulted with a more significant reduction of the TGST developed power as turbine load increases. An increase in the steam mass flow rate which leaked through the front gland seal for 5 % resulted in a decrease in TGST power for 0.38 kW, 0.43 kW and 0.70 kW at low, middle and high turbine load, respectively (values are rounded on two decimal places).

The TGST developed power values presented in Tab. 4 did not take into account turbine mechanical losses. If mechanical losses are taken into account, each value of the turbine developed power should be multiplied with turbine mechanical efficiency (the developed power will be reduced for the mechanical losses), at each observed load.

Table 4 Change in the TGST developed power at three observed loads based on the lost steam mass flow rate distribution on the front and rear gland seals

z_{front} (%)	Z_{rear} (%)	Developed turbine power (kW)		
		High Load	Middle Load	Low Load
30 %	70 %	1386.83	859.41	762.71
35 %	65 %	1386.13	858.98	762.32
40 %	60 %	1385.44	858.55	761.94
45 %	55 %	1384.74	858.12	761.56
50 %	50 %	1384.05	857.69	761.18
55 %	45 %	1383.35	857.26	760.79
60 %	40 %	1382.65	856.83	760.41
65 %	35 %	1381.96	856.40	760.03
70 %	30 %	1381.26	855.97	759.65

At each observed TGST load, the steam energy power input and output (calculated as a product of the steam mass flow rate and steam specific enthalpy) is the same, it did not depend on the distribution of the cumulative steam mass flow rate lost through the gland seals, Fig. 3. The steam energy power inputs and outputs both increase with an increase in the TGST load (from 3594.95 kW to 5479.94 kW for steam energy power inputs and from 2801.65 kW to 4048.05 kW for steam energy power outputs). The difference between the steam energy power input and output, at each observed TGST load, represents the sum of the turbine developed power, mechanical losses and energy power losses through both gland seals.

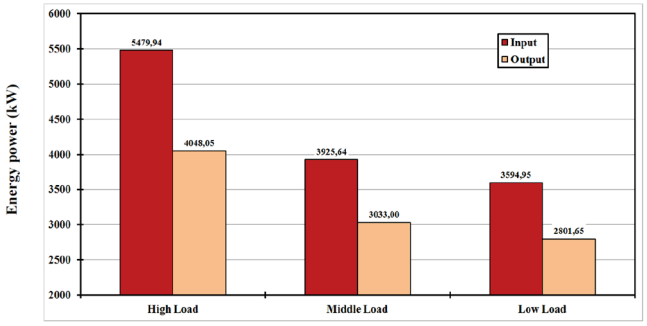

Figure 3 Steam energy power input and output of TGST at three observed loads

An increase of the steam mass flow rate lost through the TGST front gland seal (an increase in the percentage of the cumulative lost steam mass flow rate at the front gland seal) resulted in a proportional increase in the energy power loss at the front gland seal. According to the Eq. (7), the energy power loss at the TGST front gland seal is most influenced by the steam mass flow rate lost through the seal. As presented in Fig. 4, an increase of the steam mass flow rate lost through the TGST front gland seal resulted in the highest energy power losses' increase at a high turbine load (from 16.44 kW up to 38.36 kW) and the lowest energy power losses' increase at a low turbine load (from 10.78 kW up to 25.16 kW). The reason behind such occurrence can be found

in the fact that as turbine load increases, the steam mass flow rate lost through both gland seals simultaneously increases, Tab. 2.

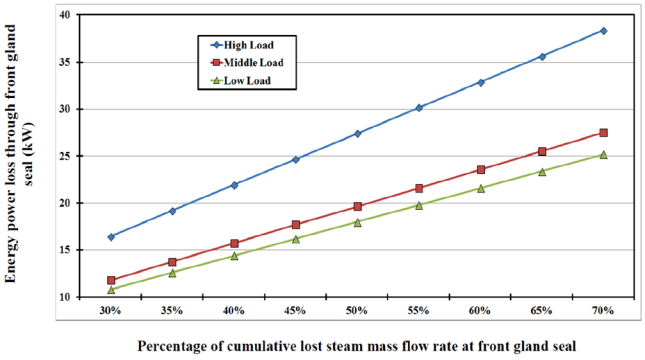

Figure 4 Energy power loss at the front gland seal in relation to the steam mass flow rate lost at the front gland seal

The analyzed distribution of the cumulative steam mass flow rate lost through both TGST gland seals resulted in the fact that an increase of the mass flow rate lost through the front gland seal simultaneously leads to a decrease in the steam mass flow rate lost through the rear gland seal and vice versa. Therefore, the energy power loss at the rear gland seal will decrease proportionally with a decrease in the steam mass flow rate which leaked through the rear gland seal, Fig. 5.

From Fig. 5, it is important to notice that a decrease in the energy power loss through the rear gland seal has the highest intensity at a high TGST load (from 28.62 kW up to 12.27 kW) and the lowest intensity at a low TGST load (from 19.81 kW up to 8.49 kW).

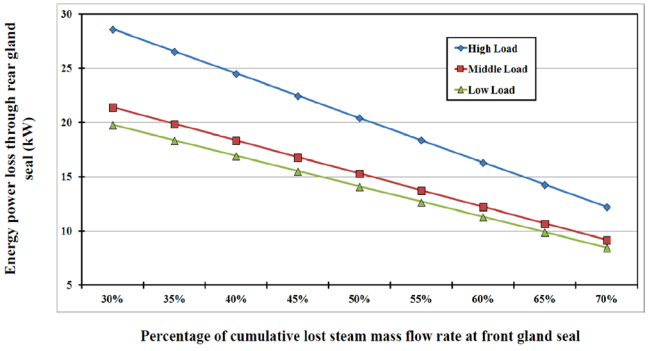

Figure 5 Energy power loss at the rear gland seal in relation to the steam mass flow rate lost at the front gland seal

A conclusion which can be derived from Fig. 4 and Fig. 5 is that the values of energy power losses through both TGST gland seals increase with an increase in turbine load. The highest influence on the values of each gland seal energy loss belongs to the leaked steam mass flow rate through the seal.

The cumulative energy power loss at both gland seals and its change with an increase in the steam mass flow rate lost through the front gland seal is presented in Fig. 6. As it can be seen in Fig. 6, an increase in the steam mass flow rate leaked through the front gland seal resulted with an increase in the cumulative energy power loss at both gland seals. An increase in the cumulative energy power loss at both gland seals has a much higher intensity at a high turbine load (from 45.06 kW up to 50.63 kW) in comparison with a middle or low turbine load (from 33.22 kW up to 36.67 kW at a middle and from 30.59 kW up to 33.65 kW at a low turbine load).

The presented change of the cumulative energy power loss at both gland seals can be explained in two ways – the first is by using Fig. 4 and Fig. 5, while the second is by using the Eq. (13). An increase in the steam mass flow rate lost through the TGST front gland seal resulted in a simultaneous increase in the energy power loss at the front gland seal, Fig. 4, and with a decrease in the energy power loss at the rear gland seal, Fig. 5. The intensity of the energy power loss increase at the front gland seal is higher than the intensity of the energy power loss decrease at the rear gland seal, which resulted in an increase in the cumulative energy power loss at both gland seals. When using the Eq. (13), an increase in the steam mass flow rate lost through the TGST front gland seal (and simultaneous decrease in the steam mass flow rate lost through the rear gland seal) will result with an increase in the cumulative energy power loss because the steam specific enthalpy at the turbine inlet is much higher than that of the steam specific enthalpy at the turbine outlet, Tab. 2.

In standard observations as well as during a conversation with the LNG carrier crew about lost steam mass flow rate through both TGST gland seals, it is concluded that approximately half of the cumulative steam mass flow rate lost through both gland seals is distributed at the front and the other half at the rear gland seal. This analysis shows that in such a distribution ratio situation, the cumulative energy power loss at both TGST gland seals will be equal to 32.12 kW at a low load, 34.95 kW at a middle load and finally 47.84 kW at a high turbine load, Fig. 6.

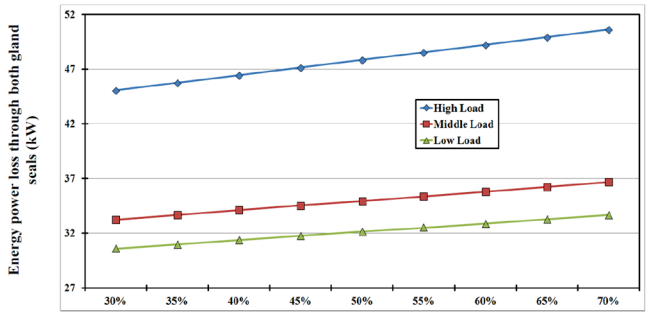

Figure 6 Cumulative energy power loss at both gland seals in relation to the steam mass flow rate lost at the front gland seal

The energy efficiency of the analyzed TGST is calculated by using the Eq. (14), and the results are presented in Fig. 7 in regards to the steam mass flow rate lost through the front turbine gland seal. The presented results of TGST energy efficiency take into account turbine mechanical losses.

An increase in the steam mass flow rate lost through the TGST front gland seal resulted in a decrease in turbine energy efficiency. The decrease in TGST energy efficiency

becomes higher and higher as turbine load increases (in the observed range of the mass flow rates lost through the front gland seal, energy efficiency decreases for 0.363 % at a low, for 0.367 % at a middle and for 0.373 % at a high load).

Energy losses which define TGST energy efficiency, taken into account in this analysis, are energy losses of the leaked steam throughout both gland seals and mechanical losses. What is not taken into account are the additional energy losses inside the turbine stages (at each stator and rotor of each stage), as well as the energy losses that are caused by the steam expansion process. According to the observed energy losses, the average value of TGST energy efficiency at a low load is 90.19 %, at a middle load 91.28 % and at a high load 92.79 %, Fig. 7.

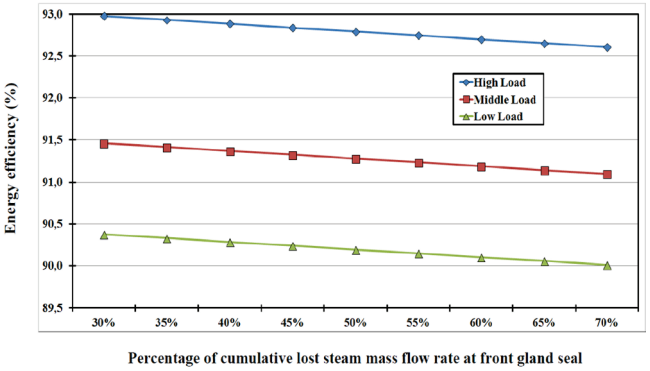

Figure 7 TGST energy efficiency change in relation to the steam mass flow rate lost at the front gland seal

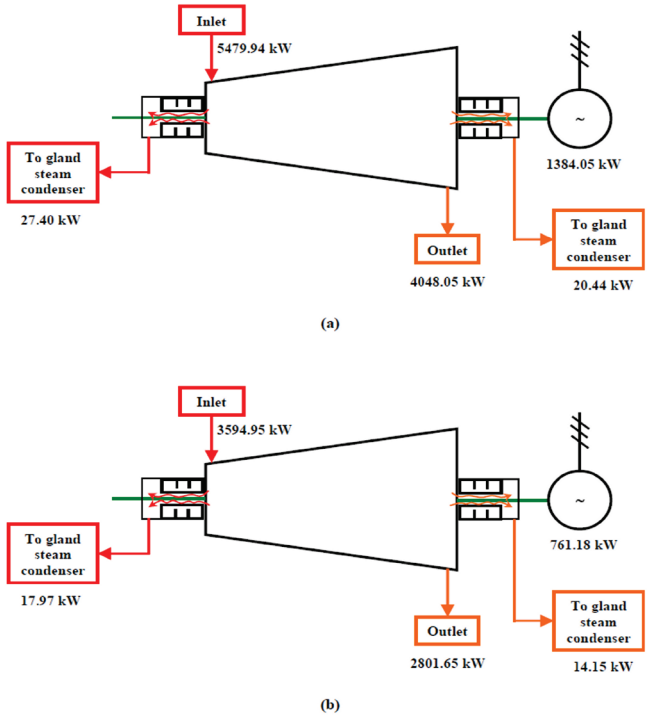

Figure 8 Energy power distribution at TGST (the cumulative lost mass flow rate distribution on the front and rear gland seal 50 % - 50 %): (a) High Load; (b) Low Load

Fig. 8 presents TGST energy power distribution at a high (a) and low (b) turbine load. The presented energy flows are based on the energy conservation equation which did not include mechanical losses. If the mechanical losses are taken into account, the turbine produced power at each load in Fig. 8 should be multiplied with mechanical efficiency (produced power will be reduced for the mechanical losses) – in that situation, mechanical losses will become an additional energy flow.

The cumulative steam mass flow rate lost through both TGST gland seals in Fig. 8 is divided in two identical parts – half is distributed on the front and half is distributed on the rear gland seal. In such a leaked mass flow rate distribution, the steam energy flow at the front gland seal is higher in comparison to the steam energy flow at the rear gland seal due to the higher steam specific enthalpy at the turbine inlet.

The recommendation for TGST operation which can be derived from the presented analysis is that TGST should operate at a high load as long as possible and the steam mass flow rate leakage through the front gland seal should be minimized. At a high load, TGST energy efficiency will be the highest, while minimization of the steam mass flow rate lost through the front gland seal will reduce TGST energy power losses.

6 CONCLUSIONS

The presented paper analyzed energy losses at the gland seals of a marine Turbo-Generator Steam Turbine (TGST). The entire analysis was performed at three different turbine loads in order to examine the energy losses at gland seals in the entire range of the steam turbine operation. The influence of change in the steam mass flow rate which leaked through the front gland seal on the TGST developed power, turbine energy power losses and energy efficiencies is researched. In the analysis, the steam turbine mechanical losses at each observed load were included. The main conclusions can be summarized in the following points:

- An increase in the steam mass flow rate which leaked through the front gland seal resulted in a decrease in the TGST developed power, in an increase in turbine cumulative energy losses and, simultaneously, in a decrease in turbine energy efficiency.
- The front gland seal should be designed with as many chambers as possible within the seal in order to reduce the leaked steam mass flow rate.
- A steam mass flow rate which leaked through the rear gland seal did not influence the TGST developed power, and at the same time, it has a low influence on the change of turbine cumulative energy losses and energy efficiencies.
- TGST load is directly proportional to the turbine developed power, cumulative energy losses and energy efficiencies – all of it increases during an increase in the turbine load.

For the analyzed TGST, it is desirable that it operates at a high load and has minimal steam mass flow rate leakage through the front gland seal. Such operation will lead to

highest energy efficiency and will decrease cumulative energy losses.

Acknowledgments

The authors would like to extend their appreciations to the main ship-owner office and the crew of the LNG carrier. This research has been supported by the Croatian Science Foundation under the project IP-2018-01-3739, CEEPUS network CIII-HR-0108, European Regional Development Fund under the grant KK.01.1.1.01.0009 (DATACROSS), the University of Rijeka scientific grant uniri-tehnic-18-275-1447 and the University of Rijeka scientific grant uniri-tehnic-18-18-1146.

NOMENCLATURE

Abbreviations:

LNG	Liquefied Natural Gas
TGST	Turbo-Generator Steam Turbine

Latin Symbols:

$\dot{E}$	power of a fluid stream, kW
h	specific enthalpy, kJ/kg
$\dot{m}$	mass flow rate, kg/s
P	power, kW
$\dot{Q}$	heat transfer, kW

Greek symbols:

η	efficiency, -

Subscripts:

en	energy
FGS	front gland seal
IN	inlet (input)
OUT	outlet (output)
PL	power loss
RGS	rear gland seal

7 REFERENCES

[1] Raptotasios, S. I., Sakellaridis, N. F., Papagiannakis, R. G., & Hountalas, D. T. (2015). Application of a multi-zone combustion model to investigate the NOx reduction potential of two-stroke marine diesel engines using EGR. *Applied Energy, 157*, 814-823. https://doi.org/10.1016/j.apenergy.2014.12.041

[2] Ryu, Y., Lee, Y., & Nam, J. (2016). Performance and emission characteristics of additives-enhanced heavy fuel oil in large two-stroke marine diesel engine. *Fuel, 182*, 850-856. https://doi.org/10.1016/j.fuel.2016.06.029

[3] Sun, X., Liang, X., Shu, G., Wang, Y., Wang, Y., & Yu, H. (2017). Effect of different combustion models and alternative fuels on two-stroke marine diesel engine performance. *Applied Thermal Engineering, 115*, 597-606. https://doi.org/10.1016/j.applthermaleng.2016.12.093

[4] Sun, X., Liang, X., Shu, G., Lin, J., Wei, H., & Zhou, P. (2018). Development of a surrogate fuel mechanism for application in two-stroke marine diesel engine. *Energy, 153*, 56-64. https://doi.org/10.1016/j.energy.2018.03.042

[5] Senčić, T., Mrzljak, V., Blecich, P., & Bonefačić, I. (2019). 2D CFD Simulation of Water Injection Strategies in a Large Marine Engine. *Journal of Marine Science and Engineering, 7*, 296. https://doi.org/10.3390/jmse7090296

[6] Mrzljak, V., Medica, V., & Bukovac, O. (2017). Quasi-dimensional diesel engine model with direct calculation of cylinder temperature and pressure. *Technical Gazette, 24*(3), 681-686. https://doi.org/10.17559/TV-20151116115801

[7] Fernández, I. A., Gómez, M. R., Gómez, J. R., & Insua, A. A. B. (2017). Review of propulsion systems on LNG carriers. *Renewable and Sustainable Energy Reviews, 67*, 1395-1411. https://doi.org/10.1016/j.rser.2016.09.095

[8] Koroglu, T. & Sogut, O. S. (2018). Conventional and Advanced Exergy Analyses of a Marine Steam Power Plant. *Energy, 163*, 392-403. https://doi.org/10.1016/j.energy.2018.08.119

[9] Ammar, N. R. (2019). Environmental and cost-effectiveness comparison of dual fuel propulsion options for emissions reduction onboard LNG carriers. *Shipbuilding, 70*(3), 61-77. https://doi.org/10.21278/brod70304

[10] Zhao, F., Yang, W., Tan, W. W., Yu, W., Yang, J., & Chou, S. K. (2016). Power management of vessel propulsion system for thrust efficiency and emissions mitigation. *Applied Energy, 161*, 124-132. https://doi.org/10.1016/j.apenergy.2015.10.022

[11] Trivyza, N. L., Rentizelas, A., & Theotokatos, G. (2018). A novel multi-objective decision support method for ship energy systems synthesis to enhance sustainability. *Energy Conversion and Management, 168*, 128-149. https://doi.org/10.1016/j.enconman.2018.04.020

[12] *Final Drawing for Generator Turbine*. (2006). Shinko Ind. Ltd., Hiroshima, Japan, internal ship documentation.

[13] Mrzljak, V., Senčić, T., & Žarković, B. (2018). Turbogenerator Steam Turbine Variation in Developed Power: Analysis of Exergy Efficiency and Exergy Destruction Change. *Modelling and Simulation in Engineering*, 2018. https://doi.org/10.1155/2018/2945325

[14] Behrendt, C. & Stoyanov, R. (2018). Operational characteristic of selected marine turbounits powered by steam from auxiliary oil-fired boilers. *New Trends in Production Engineering, 1*(1), 495-501. https://doi.org/10.2478/ntpe-2018-0061

[15] Cangioli, F., Chatterton, S., Pennacchi, P., Nettis, L., & Ciuchicchi, L. (2018). Thermo-elasto bulk-flow model for labyrinth seals in steam turbines. *Tribology International, 119*, 359-371. https://doi.org/10.1016/j.triboint.2017.11.016

[16] Lorencin, I., Anđelić, N., Mrzljak, V., & Car, Z. (2019). Exergy analysis of marine steam turbine labyrinth (gland) seals. *Scientific Journal of Maritime Research, 33*(1), 76-83. https://doi.org/10.31217/p.33.1.8

[17] Mrzljak, V. & Poljak, I. (2019). Energy Analysis of Main Propulsion Steam Turbine from Conventional LNG Carrier at Three Different Loads. *International Journal of Maritime Science & Technology "Our Sea", 66*(1), 10-18. https://doi.org/10.17818/NM/2019/1.2

[18] Naserbegi, A., Aghaie, M., Minuchehr, A., & Alahyarizadeh, Gh. (2018). A novel exergy optimization of Bushehr nuclear power plant by gravitational search algorithm (GSA). *Energy, 148*, 373-385. https://doi.org/10.1016/j.energy.2018.01.119

[19] Elhelw, M., Al Dahma, K. S., & Hamid Attia, A. E. (2019). Utilizing exergy analysis in studying the performance of steam power plant at two different operation mode. *Applied Thermal Engineering, 150*, 285-293. https://doi.org/10.1016/j.applthermaleng.2019.01.003

[20] Mrzljak, V., Poljak, I., & Medica-Viola, V. (2017). Dual fuel consumption and efficiency of marine steam generators for the propulsion of LNG carrier. *Applied Thermal Engineering, 119*, 331-346. https://doi.org/10.1016/j.applthermaleng.2017.03.078

[21] Mrzljak, V., Blecich, P., Anđelić, N., & Lorencin, I. (2019). Energy and Exergy Analyses of Forced Draft Fan for Marine Steam Propulsion System during Load Change. *Journal of Marine Science and Engineering, 7*, 381. https://doi.org/10.3390/jmse7110381
[22] Orović, J., Mrzljak, V., & Poljak, I. (2018). Efficiency and Losses Analysis of Steam Air Heater from Marine Steam Propulsion Plant. *Energies, 11*(11), 3019. https://doi.org/10.3390/en11113019
[23] Mrzljak, V., Poljak, I., & Prpić-Oršić, J. (2019). Exergy analysis of the main propulsion steam turbine from marine propulsion plant. *Shipbuilding, 70*(1), 59-77. https://doi.org/10.21278/brod70105
[24] Naserabad, S. N., Mehrpanahi, A., & Ahmadi, G. (2019). Multi-objective optimization of feed-water heater arrangement options in a steam power plant repowering. *Journal of Cleaner Production, 220*, 253-270. https://doi.org/10.1016/j.jclepro.2019.02.125
[25] Zhao, Y., Wang, C., Liu, M., Chong, D., & Yan, J. (2018). Improving operational flexibility by regulating extraction steam of high-pressure heaters on a 660 MW supercritical coal-fired power plant: A dynamic simulation. *Applied Energy, 212*, 1295-1309. https://doi.org/10.1016/j.apenergy.2018.01.017
[26] Poljak, I., Orović, J. & Mrzljak, V. (2018). Energy and Exergy Analysis of the Condensate Pump during Internal Leakage from the Marine Steam Propulsion System. *Scientific Journal of Maritime Research, 32*(2), 268-280. https://doi.org/10.31217/p.32.2.12
[27] Taylor, D. A. (1998). *Introduction to Marine Engineering*. Elsevier Butterworth-Heinemann.
[28] Mrzljak, V. (2018). Low power steam turbine energy efficiency and losses during the developed power variation. *Technical Journal, 12*(3), 174-180. https://doi.org/10.31803/tg-20180201002943
[29] Tan, H., Shan, S., Nie, Y., & Zhao, Q. (2018). A new boil-off gas re-liquefaction system for LNG carriers based on dual mixed refrigerant cycle. *Cryogenics, 92*, 84-92. https://doi.org/10.1016/j.cryogenics.2018.04.009
[30] Ahmadi, G. R. & Toghraie, D. (2016). Energy and exergy analysis of Montazeri Steam Power Plant in Iran. *Renewable and Sustainable Energy Reviews, 56*, 454-463. https://doi.org/10.1016/j.rser.2015.11.074
[31] Noroozian, A., Mohammadi, A., Bidi, M., & Ahmadi, M. H. (2017). Energy, exergy and economic analyses of a novel system to recover waste heat and water in steam power plants. *Energy Conversion and Management, 144*, 351-360. https://doi.org/10.1016/j.enconman.2017.04.067
[32] Ali, M. S., Shafique, Q. N., Kumar, D., Kumar, S., & Kumar, S. (2018). Energy and exergy analysis of a 747-MW combined cycle power plant Guddu. *International Journal of Ambient Energy*, 2018. https://doi.org/10.1080/01430750.2018.1517680
[33] Koroglu, T. & Sogut, O. S. (2017). Advanced exergy analysis of an organic Rankine cycle waste heat recovery system of a marine power plant. *Journal of Thermal Engineering, 3*(2), 1136-1148. https://doi.org/10.18186/thermal.298614
[34] Ahmadi, G., Toghraie, D., & Ali Akbari, O. (2018). Technical and environmental analysis of repowering the existing CHP system in a petrochemical plant: A case study. *Energy, 159*, 937-949. https://doi.org/10.1016/j.energy.2018.06.208
[35] Elčić, Z. (1995). *Steam turbines*. ABB, Karlovac, National and University Library Zagreb.
[36] McGeorge, H. D. (1995). *Marine Auxiliary Machinery*. 7th edition, Elsevier Science Ltd.
[37] Blažević, S., Mrzljak, V., Anđelić, N., & Car, Z. (2019). Comparison of energy flow stream and isentropic method for steam turbine energy analysis. *Acta Polytechnica, 59*(2), 109-125. https://doi.org/10.14311/AP.2019.59.0109
[38] Lemmon, E. W., Huber, M. L., & McLinden, M. O. (2010). *NIST reference fluid thermodynamic and transport properties-REFPROP*. version 9.0, User's guide, Colorado.
[39] https://www.greisinger.de (accessed: 28.10.19.)
[40] http://www.industriascontrolpro.com (accessed: 29.10.19.)
[41] http://www.krtproduct.com (accessed: 23.10.19.)
[42] Kostyuk, A. & Frolov, V. (1988). *Steam and gas turbines*. Mir Publishers, Moscow.
[43] Kanoğlu, M., Çengel, Y. A., & Dincer, I. (2012). *Efficiency Evaluation of Energy Systems*. Springer Briefs in Energy, Springer. https://10.1007/978-1-4614-2242-6

Authors' contacts:

Lino Kocijel, PhD Student
Faculty of Engineering, University of Rijeka,
Vukovarska 58, 51000 Rijeka, Croatia
E-mail: lkocijel@gmail.com

Igor Poljak, PhD, Assistant Professor
Department of Maritime Sciences, University of Zadar,
Mihovila Pavlinovića 1, 23000 Zadar, Croatia
E-mail: igor.poljak2@gmail.com

Vedran Mrzljak, PhD, Assistant Professor
(Corresponding author)
Faculty of Engineering, University of Rijeka,
Vukovarska 58, 51000 Rijeka, Croatia
E-mail: vedran.mrzljak@riteh.hr

Zlatan Car, PhD, Full Professor
Faculty of Engineering, University of Rijeka,
Vukovarska 58, 51000 Rijeka, Croatia
E-mail: zlatan.car@riteh.hr